Simple, high-performance type II β-BaB_2O_4 optical parametric oscillator

Sheng Wu, Geoffrey A. Blake, Zhaoyang Sun, and Jiwu Ling

A visible/near-IR optical parametric oscillator (OPO) based on type II phase matching in β-BaB_2O_4 (BBO) is described. Pumped at 355 nm, this OPO covers 410–2500 nm completely with a single set of standard Nd:YAG cavity optics. The output efficiency is >25%, the linewidth of the OPO is narrower than 1–2 cm^{-1} without the use of gratings or etalons, and the signal-beam divergence is <400 μrad. Three type I BBO doubling crystals are used to extend the tuning range from 208 to 415 nm. Doubling efficiencies as high as 40% are easily obtained. The reasons for the high doubling and overall system efficiency are discussed. © 1997 Optical Society of America

Key words: Type II β-barium borate optical parametric oscillator, doubling efficiency.

Optical parametric oscillators (OPO's) based on type I phase matching in β-BaB_2O_4 (BBO) crystals have been rapidly developing over the past several years. Type I BBO OPO's give high efficiency and wide tunability,[1–4] particularly when pumped at 355 nm. However, the inherent gain linewidth in type I BBO parametric oscillators varies from subnanometer to many nanometers as the wavelength is tuned toward degeneracy. For free-running type I BBO OPO's, this inconsistent linewidth precludes many applications for which sub-wave-number resolution is required. Alternative type I BBO OPO designs based on grazing-incidence gratings offer high spectral resolution, but lower efficiency. In order to generate ≥10 mJ of energy in the visible and the UV, for example, over 300 mJ of 355-nm energy is often required for pumping an OPO + OPA design (OPA is an optical parametric amplifier), which adds to the cost and complexity of such systems.[5,6] Here we describe a simple free-running OPO, based on type II phase matching in BBO crystals, that contains no frequency-selective elements yet has consistently narrow linewidth. It has a simple plano–plano cavity design, low threshold, extraordinarily high doubling efficiency, and covers the same tuning range as BBO OPO's based on type I interactions.

To the best of our knowledge, nanosecond-pulse-length OPO's based on type II phase matching in BBO crystals have been reported only once before.[7] There are two main reasons that type II BBO OPO's have not received the same wide attention as type I BBO OPO's have. First, type II phase-matched BBO crystals, although they give a consistently narrow-linewidth output, have much smaller nonlinear coefficients than BBO crystals cut for type I interactions, especially near degeneracy. Second, type II BBO crystals require much larger tuning angles than their type I counterparts in order to cover the whole tuning range when pumped at 355 nm. Therefore long- and large-aperture BBO crystals must be used to generate efficient output over the whole tuning range. In recent years, improved crystal-growing technology has made large crystals routinely available. New crystal coatings also improve performance, and, further, new cavity designs have made OPO's based on type II BBO crystals much more efficient. The OPO described in this paper reflects many of these improvements.

The cavity has a simple linear layout. As shown in Fig. 1, it consists of a plano rear mirror, M1, which is a standard metallic reflector in the near-IR, a plano output-coupling mirror, M2, which is a standard normal-incidence Nd:YAG 355-nm-high reflector, and a pump input coupler, M3, which is standard 45° high reflector for *P*-polarized 355-nm light. In the visible and the near-IR, the typical reflectivity of dielectric mirror M2 is 4%–5%, and the reflectivities of dielectric mirror M3 are 18% and 1.6% in the *S* and the *P* planes, respectively. There are two counter-rotating type II

S. Wu and G. A. Blake are with the California Institute of Technology, Pasadena, California 91125: S. Wu is with the Division of Chemistry and Chemical Engineering and G. A. Blake is with the Division of Geological and Planetary Sciences. Z. Sun and J. Ling are with Casix, Incorporated, 1933 South Myrtle Avenue, Monrovia, California 91016-4854.

Received 3 October 1996; revised manuscript received 21 January 1997.

0003-6935/97/245898-04$10.00/0

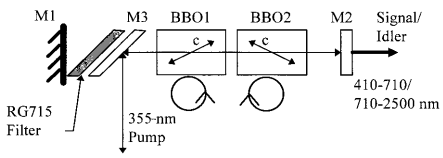

Fig. 1. Type II BBO OPO cavity, resonated on the idler wave, with two counter-rotating BBO crystals used to cover the 410–2500-nm region when pumped at 355 nm. See text for definitions of the notation.

BBO crystals inside the 7-cm-long cavity that are controlled by digital stepper motors. The 6 mm × 12 mm × 12 mm crystals, from Casix, are cut for type II phase matching at $\theta = 37°$ and $\varphi = 30°$ and are coated with a high-damage-threshold (>500 MW/cm^2 at 355 nm for nanosecond pulses) protective dielectric film, which also serves as a broadband antireflection (AR) coating. The 355-nm pump beam is *P* polarized with respect to the surface of M3, and so with type II phase matching the signal is *S* polarized while the idler is *P* polarized. A Schott RG715 long-pass glass filter is placed between rear mirror M1 and input coupler M3, which effectively absorbs >99% of the visible signal beam, thereby creating a singly resonant OPO on the idler wave.

The OPO power spectrum measured external to the cavity and without Fresnel corrections is given in Fig. 2. A Spectra-Physics GCR-16 Nd:YAG laser produces a pump beam that has a beam diameter of 5.5 mm, a pulse energy of 135 mJ, a beam divergence of less than 0.5 mrad (FWHM), and a pulse duration of 15 ns. In most of the experiments described below, the YAG 355-nm beam was left unfocused and injection seeded to provide transform-limited pump pulses. As Fig. 2 shows, the usable efficiency of the OPO is as high as 30%. We attribute this high efficiency to the following factors: pump-beam double passing, walk-off compensation inside the BBO crystals, and extra-long crystal-interaction lengths coupled with an efficient broadband AR coating. Double passing lowers the threshold energy and the intensity of this OPO design by almost[8] 50% to values near 30–40 mJ and 8–11 MW/cm^2 at the blue end of the tuning range. Near degeneracy the threshold energy rises to values of approximately 80–90 mJ for unfocused, injection-seeded 5.5-mm-diameter pump beams.

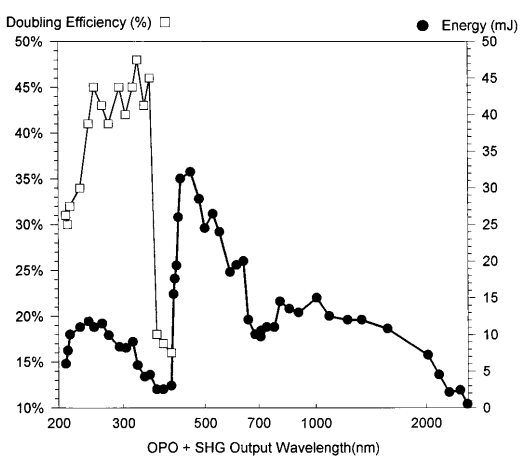

Fig. 2. Power spectrum and doubling efficiency of the 355-nm pumped type II BBO OPO when driven by an injection-seeded Spectra-Physics GCR-16 Nd:YAG laser at 135 mJ/pulse. The fundamental output of the OPO ranges from 410 to 2500 nm. Subsequent UV generation from 208 to 415 nm by second harmonic generation (SHG) is achieved in three type I BBO doubling crystals.

The walk-off compensation efficiency increase provided by the counter-rotating BBO crystals is fairly small in this idler-resonated type II BBO OPO because the idler has the same polarization as the pump, but the two-crystal design does reduce the linewidth of the OPO output because of the longer effective interaction length inside the cavity.[5] Finally, durable broadband AR coatings on the BBO crystals reduce the overall loss inside the OPO cavity and improve the lifetimes of the crystals as well.

Figure 2 demonstrates that the tuning gap at the degeneracy point (710 nm) can be easily covered with this type II OPO design. Because the signal and the idler have orthogonal polarizations, a broadband polarization beam splitter can be used to separate the signal and the idler beams near the degeneracy point quite simply. This feature has been used in the doubling experiments outlined below.

We measured the OPO's signal (410–710-nm) linewidth in a Burleigh WA-4500 pulsed wavemeter and the idler linewidth by collecting the photoacoustic absorption spectra of various gases in the near IR, the results of which are summarized in Table 1. Because of energy conservation, the linewidths of the signal and the idler are equal, being consistently narrower than 2 cm^{-1} throughout the entire tuning range when pumped by a single-frequency, injection-seeded Nd:YAG laser at twice the threshold intensity. The linewidth is less than 1 cm^{-1} when the signal wavelength is below 600 nm, as shown by the photoacoustic absorption spectrum of C_2H_2 presented in Fig. 3. When pumped with a nonseeded Nd:YAG laser ($\Delta\nu$ at 1064 nm ~1 cm^{-1}), the linewidth increases by a factor of 2, as is also demonstrated in Fig. 3. The rotational structure is nicely resolved when a seeded single-frequency pump source is used, but only barely so for an unseeded pump source. This effect, namely that the linewidth of the OPO is affected by the linewidth of the pump source, is not significant when the change in pump linewidth is small (see, for example, Ref. 7) but is clearly measurable when single-frequency versus unseeded Nd:YAG pump sources are used.

Table 1 also summarizes the high doubling efficiencies that can be obtained with this OPO design. The doubling experiments were performed in 7-mm-long AR-coated type I BBO crystals. We have observed >40% doubling efficiency for signal wavelengths from 470 to 710 nm, over 30% efficiency for doubling signal radiation from 418 to 470 nm and over 10% efficiency for doubling idler input in the 710–900-nm range. The highest efficiency obtained is 48%. These doubling efficiencies are among the highest ever reported for OPO's (the highest doubling efficiency previously obtained in BBO crystals is ~20%, while values near

Table 1. Material Parameters and Linewidth Characteristics[a]

	Wavelength Signal/Idler (nm)						
Parameter	420	500	580	660	700	780	860
Type II BBO OPO output linewidth (cm^{-1})	0.7	0.8	1.0	1.4	1.7	1.4	1.2
Linewidth acceptance (cm^{-1}, FWHM), for doubling	1.0	1.7	2.7	3.7	4.4	5.8	7.5
Angular acceptance (μrad, FWHM)	680	430	500	620	680	820	970
d_{eff} (×KDP)[b]	1.1	2.5	3.0	3.3	3.4	3.6	3.7
Doubling efficiency (%)	30	45	45	48	45	16	15

[a]The corresponding idler radiation has a linewidth comparable with the signal beam because of the conservation of energy.
[b]KDP, KH_2PO_4 crystal.

30% have been reported in KH_2PO_4 crystals[3]) and for tunable dye lasers as well, especially in the deep-UV range between 208 and 225 nm. This technology should ultimately provide a compact, efficient, and tunable deep-UV source that is finding increasing applications in many areas such as the subsequent generation of tunable vacuum-UV radiation,[9] environmental characterization,[10] material marking, and high-density photolithography.

In order to generate such high doubling efficiencies, both the linewidth and the divergence of the OPO output have to be smaller than the spectral and angular acceptance of the doubling crystal. The type II BBO OPO linewidth is consistently narrower than 2 cm^{-1}, whereas the linewidth acceptance of type I BBO doubling crystals varies from less than one wave number at 420 nm to a few wave numbers at 710 nm. Table 1 compares the linewidth acceptance of type I BBO doubling crystals with the linewidth of the type II OPO at various wavelengths throughout the tuning range. As can be seen, the OPO linewidth is always smaller than the linewidth acceptance (FWHM) of the doubling crystal. Thus no energy is wasted in the doubling process.

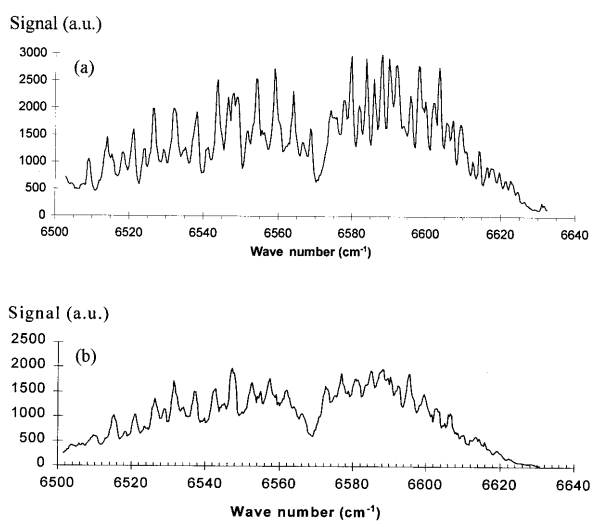

Fig. 3. (a) Photoacoustic absorption spectrum of C_2H_2 taken with a type II BBO OPO pumped at 355 nm by an injection-seeded Nd:YAG laser (whose fundamental linewidth is ~100 MHz), showing clearly resolved rotational structure. The measured linewidth of the OPO signal beam at 462 nm is approximately 0.75 cm^{-1}. (b) The same photoacoustic absorption spectrum of C_2H_2 now taken with a type II BBO OPO pumped by an unseeded Nd:YAG laser (with a linewidth of ~1 cm^{-1}). Here the rotational structure of C_2H_2 is only barely discernible, and the signal-to-noise ratio drops as the linewidth goes up. The measured signal linewidth is now ~2 cm^{-1}.

As noted above, the divergence of the OPO output must also be smaller than the angular acceptance (FWHM) of the doubling crystals if efficient doubling is to be achieved. It is well known that in a plano–plano cavity the beam divergence of the nonresonated part, be it idler or signal, will be substantially reduced. For example, Orr *et al.*[11] have observed the divergence for the idler from a plano–plano signal resonant type I BBO cavity to be so small that it is indistinguishable from the pump, or even smaller. Similar cavities resonated on the idler also possess very small signal-beam divergences. We have, for example, achieved less than 0.5-mrad divergence for the signal in a type I BBO OPO system, with a doubling efficiency (of over 18%) that is limited primarily by the fact that the linewidth of a type I BBO OPO is larger than the linewidth acceptance of the doubling crystal.[12] In the present work on an idler-resonated type II BBO OPO, we have observed less than 400-μrad signal-beam divergence in the sensitive plane of the doubling crystal. This divergence is smaller than the angular acceptance of BBO type I doubling crystals throughout the OPO tuning range. The divergence of the signal in the insensitive plane of the doubling crystal is ~600 μrad when the signal is less than 600 nm and increases to >2 mrad at the degeneracy. This relatively large divergence in the insensitive plane of the doubling crystal does not affect the doubling efficiency because the acceptance angle in the insensitive plane is even larger.

At the blue end of the tuning range, the doubling efficiency drops below 40% because the d_{eff} of BBO crystals decreases below 460 nm, as is summarized in Table 1. The doubling efficiency of the idler (710–840 nm) is just over 10% because its divergence is ≥2 mrad in the sensitive plane of the BBO doubling crystal, which is larger than its angular acceptance. Be-

cause the divergence of the idler in the other direction is as small as that found for the signal, the doubling efficiency of idler radiation can be improved when a zero-order half-wave plate is used to rotate the polarization of the idler 90°, thereby greatly reducing the idler divergence in the sensitive plane of the BBO doubling crystal.

We conclude with speculations on why the divergence of the nonresonated wave in a singly resonant plano–plano OPO cavity is so small. To our knowledge, this phenomenom has not been well explained despite having been observed many times. Because the nonresonated wave obtains all its energy in a single pass, its beam quality will be dictated by the beam quality of both the pump and the resonated wave. From Ref. 13, the steady-state equation for obtaining the beam diameter of the resonated wave inside a singly resonant plano–plano oscillator is given by

$$\left(\frac{\pi}{2L\lambda_S}\right)^2 \varpi_s^{\,6} + \varpi_s^{\,2} - \omega_p^{\,2}/2 = 0,$$

where $\varpi_s = \omega_s$ are beam waists under steady-state conditions, L is the cavity length, and the subscripts i, s, and p denote the idler, signal, and pump fields, respectively. Note that in the formalism used here, idler refers to the wave that is not resonated and signal refers to the resonated wave.

From the above equation, we note that the smaller the resonating wave's wavelength (λ_s) becomes, the smaller the steady-state ω_s will be, and for a Gaussian beam (in the far field, all three waves will have Gaussian profiles), a larger beam divergence will result. Thus if the longer wavelength part of the OPO output is chosen as the resonated wave, a smaller output divergence is obtained.

At the same time, the acceptance angle of the OPO crystal(s) may also begin to limit the divergence of both the resonated and the nonresonated waves. Furthermore, because of phase-matching restrictions, if the longer wavelength side of the degeneracy point is resonated, a smaller divergence for the nonresonated wave is produced. Phase-matching restrictions also explain the fact that the divergence of the signal in the insensitive plane increases as it goes toward degeneracy, whereas the divergence of the signal in the sensitive plane stays the same because it is always constrained by the acceptance angle of the type II BBO crystals. Numerical simulations are currently being developed to examine these phenomena quantitatively.[12]

To summarize, a simple, compact optical parametric oscillator (OPO) with a nearly constant linewidth of 1–2 cm^{-1} across the entire visible/near-IR region of 410–2500 nm is described. This OPO design, based on type II phase matching in 355-nm pumped BBO, uses only standard Nd:YAG cavity components and contains no frequency-selective elements beyond the BBO crystals themselves. Singly resonant operation on the idler wave leads to very low signal-beam divergences and high doubling efficiencies, attributes that are important for many applications requiring tunable UV radiation. The rugged, compact nature of the type II BBO cavity coupled with its consistently narrow linewidth provides an alternative to the more complex master OPO/slave OPA approach that is most common among narrow-band commercial systems.

This research was supported in part by a U.S. Defense Advanced Research Project Agency/U.S. Office of Naval Research University Research Initiative grant to the California Institute of Technology. The authors also gratefully acknowledge additional instrumentation support from the Infrared, Submillimeter, and Radio Astronomy/Exobiology Programs at NASA and the Experimental Physical Chemistry Program of the U.S. National Science Foundation.

References and Notes

1. L. K. Cheng, W. R. Bosenberg, and C. L. Tang, "Broadly tunable optical parametric oscillation in β-BaB_2O_4," Appl. Phys. Lett. **53,** 175–177 (1988).
2. Y. X. Fan, R. C. Eckardt, R. L. Byer, J. Nolting, and R. Wallenstein, "Visible β-BaB_2O_4 optical parametric oscillator pumped at 355 nm by a single-axial mode pulsed source," Appl. Phys. Lett. **53,** 20–2016 (1988).
3. H. Komine, "Optical parametric oscillation in a beta-borate crystal pumped by an XeCl excimer laser," Opt. Lett. **13,** 643–645 (1988).
4. A. Fix, T. Schroder, R. Wallenstein, J. G. Haub, M. J. Johnson, and B. J. Orr, "Tunable beta-barium borate optical parametric oscillator: operating characteristics with and without injection seeding," J. Opt. Soc. Am. B **10,** 1744–1750 (1993).
5. W. R. Bosenberg, W. S. Pelouch, and C. L. Tang, "High-efficiency and narrow linewidth operation of a 2-crystal β-BaB_2O_4 optical parametric oscillator," Appl. Phys. Lett. **55,** 1952–1954 (1989).
6. B. C. Johnson, V. J. Newell, J. B. Clark, and E. S. McPhee, "Narrow-bandwidth low-divergence optical parametric oscillator for nonlinear frequency-conversion applications," J. Opt. Soc. Am. B **12,** 2122–2127 (1995).
7. W. R. Bosenberg and C. L. Tang, "Type-II phase matching in a beta-barium borate optical parametric oscillator," Appl. Phys. Lett. **56,** 1819–1821 (1990).
8. Y. Wang, Z. Xu, D. Deng, W. Zheng, X. Liu, B. Wu, and C. Chen, "Highly efficient visible and infrared β-BaB_2O_4 optical parametric oscillator with pump reflection," Appl. Phys. Lett. **58,** 1462–1463 (1991).
9. J. P. Marangos, N. Shen, H. Ma, M. H. R. Hutchinson, and J. P. Connerade, "Broadly tunable vacuum-ultraviolet radiation source employing resonant enhanced sum–difference frequency mixing in krypton," J. Opt. Soc. Am. B **7,** 1254–1259 (1990).
10. P. O. Wennberg, R. C. Cohen, N. L. Hazen, L. B. Lapson, N. T. Allen, T. F. Hanisco, J. F. Oliver, N. W. Lanham, J. N. Demusz, and J. G. Anderson, "An aircraft-borne laser induced fluorescence instrument for the *in situ* detection of hydroxyl and hydroperoxyl radicals," Rev. Sci. Instrum. **65,** 1858–2550 (1994).
11. B. J. Orr, M. J. Johnson, and J. G. Haub, "Spectroscopic applications of pulsed tunable parametric oscillators," in *Tunable Laser Applications*, F. J. Duarte, ed. (Marcel Dekker, New York, 1995), pp. 11–83.
12. S. Wu, G. A. Blake, Z. Sun, and J. Ling are preparing the following paper for publication: "Beam quality in nanosecond-pulsed optical parametric oscillators."
13. S. J. Brosnan and R. L. Byer, "Optical parametric oscillator threshold and linewidth studies," IEEE J. Quantum Electron. **QE-15,** 415–422 (1979).